Title

THE MEASUREMENT OF RADIATION DAMAGE IN ORGANIC MATERIALS IN THE RANGE OF ELECTRON ENERGY BETWEEN 200 KeV AND 650 KeV

Author

Howitt, David George.

Publication Date

1974-12-01

LBL-3180
c.1

THE MEASUREMENT OF RADIATION DAMAGE IN ORGANIC MATERIALS IN THE RANGE OF ELECTRON ENERGY BETWEEN 200 KeV AND 650 KeV

David George Howitt
(M. S. thesis)

December, 1974

Prepared for the U. S. Atomic Energy Commission
under Contract W-7405-ENG-48

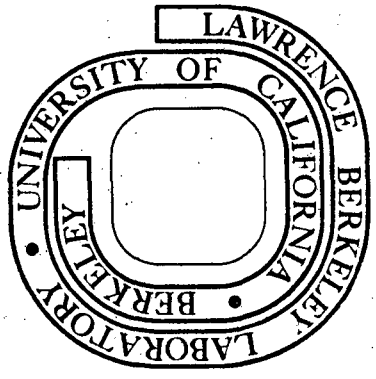

LBL-3180
c.1

DISCLAIMER

Table of Contents

THE MEASUREMENT OF RADIATION DAMAGE IN ORGANIC MATERIALS IN THE RANGE OF ELECTRON ENERGY BETWEEN 200 KeV AND 650 KeV

David George Howitt

Inorganic Materials Research Division, Lawrence Berkeley Laboratory and Department of Materials Science and Engineering, College of Engineering; University of California, Berkeley, California

ABSTRACT

The following treatise is an account of the studies performed concerning the radiosensitivities of two organic compounds to electron irradiation at energies in the range from 200 KeV to 650 KeV. The radiosensitivities were standardized according to the loss of crystallinity of the material which was monitored from it's diffracting properties, after techniques had been devised so as to measure the electron doses.

From the results obtained, conclusions can be drawn as to the applicability of high voltage transmission electron microscopy techniques to the detailed study of these materials and to the general behavior of organic solids. The results indicate that the radiosensitivities of these materials are decreased by approximately 50 percent over this total energy range.

I. INTRODUCTION

The radiosensitivity of the majority of organic materials to electrons of high energy is such, that there is little useful application that can be made of conventional electron microscopy techniques at high resolution.

That is to say, the degradation rate of the high resolution fourier components, contributing to the image of the crystalline material, is so rapid, that in an electron exposure sufficient to record them, the structure they afford is destroyed.

An extensive and complete review of the limitations that these high radiosensitivities impose upon the application of transmission electron microscopy is given by Glaeser (1973) and will not therefore be reviewed in detail. The conclusions indicate, however, that many organic materials are within the range of applicability, if techniques can be found to decrease their respective radiosensitivities by an order of magnitude or less.

Experimental observations (Glaeser and Hobbs)(Siegel 1972) appear to indicate that the radiosensitivities of various representative types of organic material are not reduced by this amount even at liquid helium temperatures; and hence as an alternative, the advantages of the energy dependence upon these radiosensitivities has been investigated.

II. THE ENERGY LOSS AND DISSIPATION PROCESS CHARACTERISTIC OF RADIATION FROM THE ELECTRON MICROSCOPE

It is well known that in the traversing of matter by high energy electrons, moderation occurs almost entirely through energy losses to the electronic system of the atoms and molecules making up the medium, whilst at very high energies Bremsstrahlung (radiation loss) becomes the important energy loss mechanism.

Bethe and Heitler (1934) estimated the relative contributions of these losses to collision losses, an appropriate expression being:

$$\frac{\left(\frac{dE}{dx}\ \text{radiative}\right)}{\left(\frac{dE}{dx}\ \text{collision}\right)} = \frac{EZ}{800}$$

where E is the total energy (kinetic energy + rest mass) measured in MeV.

Thus in considering the organic materials employed in the proceeding investigations, where the atomic numbers (Z) average between 1 and 16, we may employ with little error the relativistic stopping power formula for electrons due to Bethe (1933), where radiation losses are ignored i.e.

$$\frac{-dE}{dx} = \frac{N\cdot 2\pi e^4\cdot Z}{mv^2}\left[\ln\frac{mv^2E}{2I^2(1-\beta^2)} - (2\sqrt{1-\beta^2} - 1 + \beta^2)\ln 2 + 1-\beta^2 + \frac{1}{8}(1-\sqrt{1-\beta^2})^2\right] \qquad (1)$$

where

N = Number density = the number of atoms/unit volume in the absorbing material

Z = The averaged atomic number of the sample as a whole

e = The electronic charge

m = The electron rest mass

v = The electron velocity

β = the electron velocity/the velocity of light

and I is the mean excitation energy, the main parameter with respect to the medium in this equation. This parameter has been calculated for a few simple atoms but is usually experimentally derived.

Bloch (1933) and Lindhard and Scharff (1953), using statistical atomic models have shown that $I \approx zk$ where k is a constant. In the materials studied here, a value of 13 for k would seem appropriate from the data of Fano (1964) assuming that stopping power is merely an additive function of the constitutive atoms.

From the nature of the Bethe equation one would therefore expect the dependence of the energy loss rate of the incident electrons, and hence the radiosensitivity of the exposed material, to approximate a $1/v^2$ relation, following the behavior of the leading term, for very thin specimens.

It should, of course, be noted that the energy loss of the electron beam need not be simply related to the damage suffered by the material, since the excited molecules resulting from the primary

electronic interactions may dissipate their energy through a variety of processes including secondary ionizations and non-destructive decay.

Thus, the cross-section for damage may be greater or smaller than the ionizing cross-section σ_i where an appropriate expression is

$$\sigma_i = -(NW)^{-1} \frac{dE}{dx} \qquad (2)$$

where W is the average energy loss per ionization.

The effects of direct displacement and their contribution to the damage cross-section (σ_d) are for the range of electron energies considered here, negligible. Only in materials such as hexadecachlorophthalocyanine, which can support electron exposures greater than 10 coulombs/cm^2 does the total damage cross-section have a sufficiently small value to warrant comparison with the cross-section for "knock on" processes.

Electron spin resonance studies (Burge and Smith, 1962) show that for saturated organic compounds, typically one change in the molecular structure occurs as the result of each ionization, hence to a reasonable approximation in l-valine the damage cross-section might be equated to that of the ionization cross-section,which represents the significant component of the inelastic scattering cross-section as far as the radiation damage process in concerned.

It has been the purpose of this investigation to observe the experimental behavior of the damage cross-section in two organic materials, l-valine and adenosine, in the energy range from 200 KeV to

650 KeV and to establish the existance of any inconsistencies in equating it directly with the inelastic scattering cross-section.

III. THE ELECTRON MICROSCOPY OF BEAM SENSITIVE MATERIALS

A. The Optimization of Conditions

In the formation of a meaningful high resolution fourier or point-to-point image of a specimen in an electron microscope, it is often assumed that the electrons which suffer inelastic collisions can contribute only noise, the only electrons contributing to the signal being those which have suffered elastic collisions. This is, in fact, not the case, for an inelastically scattered electron can be accurately refocussed into the image and is associated with flawed representation only when it suffers a further collision, elastic or inelastic.

In the case of radiosensitive materials where effectively all the damage is caused by inelastic collisions, the importance of a low inelastic/elastic cross section ratio is obvious. Not so obvious is the advantage that can be gained from obtaining signal from the inelastically scattered electrons if both cross-sections, elastic and inelastic, are reduced such that the probability of an electron suffering two collisions is almost negligible. This advantage may be substantial since $\sigma_e < \sigma_i$, and conventionally the signal contribution from σ_i is small.

When considering radiosensitive materials, it is also important to consider the efficiency of the detecting device since a minimal exposure of the specimen is desirable. The effects of electron energy upon some relevant photographic emulsions have been considered by Cosslett et al. (1974) who concluded that the loss in sensitivity of

the emulsion with increasing energy, which varies as its inelastic cross section, can be compensated for by the increase in its resolution. Thus, even with conventional emulsions, one need not suffer any disadvantage in recording efficiency since comparable detail can be recorded at proportionately lower magnifications with increasing electron energy.

The detecting efficiency of the emulsion or its total sensitivity can of course be improved by increasing its thickness (Jones and Cosslett, 1970) and the detecting efficiency might be improved to a limit, where the positional deviation or straggling of the electron from its initial coordinates affects the detectable detail from the negative.

Thus, in general where the image is photographically recorded directly, any decrease in the cross-section for radiation damage, with increasing electron energy, can be regarded as significant since the cross section for damage and probability of detection do not vary proportionately. Hence the analysis of Breedlove and Trammel (1970) indicating the insensitivity of the σ_i/σ_e ratio suggests for the case where the detector is a suitable photographic emulsion that the proportion of damage sustained to record an image will decrease with increasing energy.

Values for the cross-section for elastic scattering can be calculated from the optical theorem (Schiff 1956) as

$$\sigma_e = 2\lambda I_m\{F_{sp}(0)\} \qquad (3)$$

Where $I_m\{F_{sp}(0)\}$ represents the imaginary part of the complex scattering amplitude, calculated from the phase grating approximation (or strong phase approximation). For a single scattering atom such an expression is rigorously correct since this represents an exact summation of the infinite Born series at small scattering angles (Chiu and Glaeser 1973).

B. The Critical Exposure

It is convenient in many cases to describe the radiosensitivity of an organic compound in terms of the critical exposure, which is the electron dose per unit area a material can support before suffering complete loss of crystallinity. Such a measure may be of course a function of thickness and therefore is a rather non-rigorous parameter. When applied to very thin specimens however, whose thickness is very much less than the penetration distance, or range of the radiation, the energy loss rate dE/dx is very nearly constant though the specimen.

Therefore the critical exposure in this case, is the number of electrons that must pass through the specimen to effect complete disorder. Only a proportion of these electrons in fact lose significant energy, however, we may regard each electron as loosing energy in the sample at a rate -dE/dx and write the total energy imparted to the specimen to effect its destruction as

$$E_T = \eta \cdot \frac{dE}{dx} \mu \tag{4}$$

where μ is the specimen thickness and η the critical exposure or

$$\frac{E_T}{\mu} = E_\mu = \eta \frac{dE}{dx}$$

when E_μ is the total energy imparted per unit depth.

Thus, if the total energy required to effect disorder is not dependent upon electron energy, we would expect to have a dependence of critical exposure of the form $\eta = \kappa(dE/dx)^{-1}$ where κ is a constant. If we employ the non-relativistic expression for dE/dx where ε is the base of natural logarithms, we obtain

$$\eta = \kappa \left[\frac{N \cdot 4\pi e^2 Z}{mV^2} \ln \left\{ \frac{mV^2}{2I} \sqrt{\frac{\varepsilon}{2}} \right\} \right]^{-1} \tag{5}$$

equivalent to a β^2 dependance. (Eq. 1)

If however E_T is a function of electron energy such that the damage mechanism is specific to particular energies then we expect a relation of the form

$$\eta = E_\mu(E) \left(\frac{dE}{dx}\right)^{-1} \tag{6}$$

which will not be consistent with the previous description. This situation can of course be considered in terms of

$$\sigma_d = -\frac{1}{NW_d} \cdot \frac{dE}{dx} \tag{7}$$

where W_d, the average energy loss per damage event, is dependent upon the electron energy, when the damage mechanism is specific to particular energies.

IV. THE MEASUREMENT OF THE ENERGY DEPENDENCE OF RADIATION DAMAGE

In this investigation the variation of critical exposure with incident electron energy was determined in the range 200-650 KeV for two organic compounds, the aliphatic amino acid l-valine (plate I) and the ribonucleoside adenosine (plate II) over a range of dose rates. The dose rates were determined simultaneously using an efficient faraday cup and a lithium drifted silicon detector. (Appendix I) employing the indistinguishability of the materials diffraction pattern as an end point (plate III).

The measurement of beam currents in the final image plane of the Berkeley 650 Kv microscope (D_{screen}) is not straightforward, since it is found that for fixed beam currents at the specimen ($D_{specimen}$) the expected magnification relation, $D_{screen} = D_{specimen}/M^2$ where M is the linear magnification, is not obeyed. In fact at magnifications greater that 10 K, at all energies, this relation was not accurately approached and the current density in the image plane increased inconsistently with increasing magnification.

This effect of additional electron incidence at the image plane from electrons not originating from the associated object is not uncommon in high voltage microscopes and arises from the malalignment of lens apertures and the back-scattered electrons (created on the walls of the microscope column) being able to reach the final image.

The contribution from these additional electrons is difficult to estimate since there is no accurate qualitative way to distinguish

them. Their presence can be observed in the broad distribution of the pulse height spectrum from the silicon detector (Figs. IV and VII) and some can be removed by introducing intermediate apertures. Thus since this effect is not clearly distinguishable it is only possible to estimate its contribution and since this contribution is to some extent dependent upon the condenser lens setting a simple but accurate correction is not possible.

The variation of the predicted beam current density at the specimen with magnification is shown, for nominal condenser settings at the three electron energies investigated, in Fig. I. It is apparent that this effect is capable of introducing errors of 50 percent in relatively low magnification ranges. To reduce the error from this effect only the low magnification ranges were used, however even here errors of 5 percent may be expected, depending upon the condenser excitation. In the 200 Kv range of this microscope the range of the objective lens is not sufficient to enable the image to be accurately focussed above 15 K and hence measurements at magnifications above this were avoided.

V. THE ENERGY DEPENDENCE OF RADIATION DAMAGE IN L-VALINE AND ADENOSINE

Despite these limitations, reasonable estimations of the critical exposures for l-valine and adenosine were obtained at three electron energies. The exposure lifetime variations are shown in Figs. II to IV.

It is interesting to note that both l-valine and adenosine show some deviation from the reciprocity relation at high beam currents. This could be interpreted as being due to a beam heating effect; however it should be remembered that in order to obtain high current densities, the second condenser lens approaches a focussed condition where the influence of any nonuniformity in the beam profile might become evident. Thus, since the fading diffraction pattern technique will monitor the behavior of the less heavily irradiated portions of the specimen, the detector will overestimate whenever the specimen is non-uniformly irradiated. Similary at such beam diameters any small condenser instability or beam drifting will become evident and may cause the beam current measurement to differ from its actual value, hence the long lifetime measurements were considered more reliable. The values obtained for the critical exposure, from extrapolation of these curves yields the following for the the two materials.

	650 KV	350 KV	200 KV
L-valine	$10.0\pm1.0\times10^{-3}$ A/cm^2	$8.0\pm0.8\times10^{-3}$ A/cm^2	$5.0\pm0.5\times10^{-3}$ A/cm^2
Adenosine	$6.0\pm0.6\times10^{-2}$ A/cm^2	$4.5\pm0.5\times10^{-2}$ A/cm^2	$2.8\pm0.3\times10^{-2}$ A/cm^2

An error of 10 percent is appropriate since there were variations of about 5 percent in the values of the lifetimes obtained at specific current densities.

These values of critical exposure are shown in relation to the electron velocity in Fig. V. The slope of a β^2 relation is shown in the diagram for comparison, l-valine was found to obey a $\beta^{2.8}$ and adenosine a $\beta^{3.0}$ relation.

VI. DISCUSSION

In order to calculate the G value, the number of molecules damaged per 100 eV of energy imparted to the specimen, the value for -dE/dx, the energy lost by the beam in traversing the specimen, should be obtained and compared with the extent of radiation damage.

Assuming that 63 percent of the specimen has been destroyed at a molecular level when no crystallinity is detectable from its diffraction pattern, or equivalently that all the molecules have received one hit then

$$G = \frac{\text{The molecular density} \times 0.63 \times 100}{N_{cr}\ dE/dx} \qquad (8)$$

Where N_{cr} is the number of electron required to completely destroy the diffraction pattern of the specimen per unit area (the critical exposure in electrons).

Taking appropriate values for the quantities in the expressions for dE/dx, where for l-valine $N=1.23\times10^{23}$ cm^{-3} (Torri and Iitaka, 1970) $Z=6.17$ and $I=1.28\times10^{-10}$ ergs. and for adenosine $N=1.106\times10^{23}$ (Lai 1969) $Z=8.35$ and $I=1.74\times10^{-10}$ ergs, the respective G values and the average energy to destroy a molecule can be calculated.

Similarly, the calculation of the ionizing cross-section from Eq. (2) is possible, assuming an appropriate value for the average energy loss per ionization, taken to be 50 eV (Rauth and Simpson 1964). Further by equating N_{cr} with the D_{37} dose the damage cross section can be conveniently taken as $1/N_{cr}$.

The values for all these quantities are displayed in Table I for both l-valine and adenosine at the three electron energies considered. From the comparison of the ionization cross sections with the elastic scattering cross sections for carbon at the same electron energy (Chiu, private communication) we obtain for l-valine.

	$\sigma_i \times 10^{-19}$	$\sigma_e \times 10^{-19}$	σ_i/σ_e
650 kv	7.28 cm^2	1.46 cm^2	4.99
350 kv	8.36 cm^2	2.26 cm^2	3.70
200 kv	10.4 cm^2	3.46 cm^2	3.01

and for adenosine

	$\sigma_i \times 10^{-19}$	$\sigma_e \times 10^{-19}$	σ_i/σ_e
650 kv	9.59 cm^2	1.46 cm^2	6.57
350 kv	10.9 cm^2	2.26 cm^2	4.82
200 kv	13.2 cm^2	3.46 cm^2	3.81

which indicates that the proportion of elastic scattering decreases with increasing energy.

The comparison of the damage cross section with the ionization cross section at these three energies are for l-valine

	$\sigma_d \times 10^{-17}$	$\sigma_i \times 10^{-19}$	σ_d/σ_i
650 kv	1.6 ± 0.2 cm^2	7.28 cm^2	21.9 ± 2.2
350 kv	2.0 ± 0.2 cm^2	8.36 cm^2	23.9 ± 2.4
200 kv	3.2 ± 0.3 cm^2	10.9 cm^2	30.8 ± 3.1

and for adenosine

	$\sigma_d \times 10^{-18}$	$\sigma_i \times 10^{-19}$	σ_d/σ_i
650 kv	2.67 ± 0.3 cm^2	9.59 cm^2	2.8 ± 0.3
350 kv	3.56 ± 0.4 cm^2	10.9 cm^2	3.2 ± 0.3
200 kv	5.71 ± 0.6 cm^2	13.2 cm^2	4.3 ± 0.4

Thus the data presented here indicates that the damage cross section decreases faster than the ionizing cross section but at about the same rate as the elastic cross section with increasing energy.

The equating of the behavior of the damage cross section with that of the ionizing cross section in this energy range might therefore give rise to an error of about 25 percent. This might be interpreted as 25 percent of the damage reaction which follows ionization being suppressed at 650 KeV or 25 percent of such events that at the lower energy do not recombine doing so at the highest energy.

The consistency of the behavior of the damage cross section in both materials, despite their difference in structure and the mean free paths of the damage events differing by almost an order of magnitude, suggests that the behavior is not dominated by a particular damage event. In addition the increase in the mean free path between the damage events, with increasing energy, is not consistent with an increased overlapping of recombination volumes.

Indeed such behavior would suggest that the damage mechanism might be a complicated process requiring some interaction of events or rather of formed species, the decrease in the proximity of the events being the cause for this decrease. Such behavior would be consistent with

the deviation from the reciprocity relation of the lifetime beam current density curves, where at high levels of illumination the radiation damage process might be accelerated due to the increase in the density of events.

Thus it would appear that a single hit target explanation of the damage process is not completely adequate and that the structural disintegration of the material may be at least partially due to the interaction of free radicals, or cross linking, rather than of scission events arising from a single interaction. The comparison of the ionizing cross section and average damage cross section implying a single-hit process might therefore, although reasonable in its approximation, be inherently misleading.

That the damage cross section ($1/N_{cr}$) is much larger than the ionizing cross section might also be misleading, suggesting intense secondary ionization. However since the technique of selected area diffraction is not capable of distinguishing order at the atomic level, such as the perservation of a single bond, we must consider that the damage cross section measured here is an average cross section for events which degrade the material to a limit of distinguishability not to complete destruction. Comparison with the E.S.R. data of Burge and Smith (1962), who find an approximate equality between σ_i and σ_d, in materials similar to l-valine, indicates a discrepency of about a factor of 30. Since their technique is not subject to limitations of detectability, we might interpret this as the fading diffraction pattern technique distinguishing a single damage event as the loss

of coherence within the matrix of a region 30 atoms in volume. In l-valine since these are 19 atoms per molecule, the selected area diffraction technique yields a damage cross-section comparable to the damage cross section offered by a molecule.

The behavior of the damage cross seciton should nevertheless be consistant with the behavior of the true damage cross section which would represent the average area offered by each atom for the precipitation of atomic rearrangement.

Thus the consistancy in the behavior of the damage cross section between 200 keV and 650 keV in l-valine and adenosine suggests that the damage mechanisms are similar, and the 25 percent decrease in damage cross section normalized to stopping power in both these materials, suggests that a model accounting for free radical interactions is appropriate.

A quantitative assessment of the significance of these effects, in terms of increased resolution in the image plane of an electron microscope, requires that we estimate from them, the proportions of signal and noise events for the thickness of specimen used and the resolution required. Thus the change in the image characteristics for the electron dose that degrades the sample to that resolution can be determined with respect to electron energy variations.

In the case of l-valine and adenosine however, the critical exposure is limiting to such a degree that at the resolution it permits, almost all the electrons leaving a thin specimen can be considered as signal. Thus the statistical noise in this limited signal becomes the limit to resolution.

For any element R×R cm^2 we have $R^2 N_{cr} f$ electrons exciting the photographic emulsion where f represents the collection efficiency of the emulsion. In order to resolve the dimension R in the absence of image processing we require a signal to noise ratio of 5 (Rose 1948) and must therefore satisfy

$$t \cdot N_{cr} R^2 > 5\sqrt{N_{cr} f R^2}$$

$$\text{i.e} \qquad R > 5/\sqrt{f\, N_{cr}} \tag{9}$$

which is equivalent to the form of the equation used by Glaeser (1973) to predict the resolution obtainable in radiosensitive materials ignoring requirements of contrast. Since f is effectively constant for certain commercial emulsions (Coslett 1974) we may calculate, taking f=0.25 and demanding 10 percent contrast the difference in the expected resolution. From such calculation our anticipated resolution increase from 57Å to 40Å in l-valine and from 24Å to 16Å in adenosine from 200 kv to 650 kv.

APPENDIX I

A Comparison of the Measurement of Beam Current Densities in an Electron Microscope Using a Faraday Cup and Solid State Detector.

In order to make a precise estimate of the electron density incident upon a confined region of the object plane of an electron microscope it is necessary to measure it directly, which can only be achieved by sampling the electron density in an image plane.

The most attractive of these planes to introduce a measuring device into is the final image plane since here its presence need not interfere with the normal operation of the microscope and the area of interest can be easily defined.

The large magnifications of the final image plane, and hence the low current densities to be measured, commonly deter from the use of a primary faraday cup as the measuring device and favors either solid state detectors, which operate most efficiently at electron densities less than 10^{-12} amperes/cm^2 or photographic exposure meters which have large areas of capture but ranges limited to somewhat higher electron intensities. The accuracy of such detectors in predicting an absolute measure of the current density are of course limited by the accuracy of the standardising faraday cup at such levels of intensity, since the errors introduced from a magnification extrapolation, where the devices are situated at significantly different positions in an electron microscope, will be very large.

The detection of small collected currents itself represents no problem; however at electron incidence levels such as 10^{-14} amperes/cm^2 the effects of leakage and current generation from insulators or external fields surrounding the collector will introduce significant error. Thus somewhat severe restrictions are imposed upon the prefabrication and operation of a faraday cup of this type.

A faraday cup capable of being introduced into the camera chamber of an electron microscope has been constructed to operate in conjunction with a Cary electrometer, capable of measuring currents of 10^{-17} amperes. In order to reduce the effects due to spurious current generation the cup is surrounded by an annealed mu metal shield and the insulators are constructed from prefired and carefully machined alumina. To reduce leakage effects to a minimum the cup is supported only at its base by these insulators and has only one connection which is a direct contact to the electrometer. Geometrically the cup is effectively infinitely long, being in the shape of a tall cylinder of length twenty times its width and to reduce the effects of backscattering to a minimum it is constructed of solid carbon. Thus only primarily backscattered electrons should be lost introducing an error of less than one percent (Grubb 1970). The cup and housing are shown in plates 4 and 5.

Following installation, the magnitude of the background current drift from the cup was less than 10^{-15} amperes, an order of magnitude greater than the background current drift from the electrometer itself. Thus using a defining aperture of 0.18 cm^2 this corresponds to an

error of less than 5.6×10^{-15} amperes/cm^2 in the determination of the beam current collected by the cup.

The cup was used in conjunction with a lithium drifted silicon detector, designed to record 650 KeV electrons, both having defining apertures in the same plane and being able to operate simultaneously. The detectors were compared using 650 Kv and 350 Kv electrons over a range of current densities at the detectors. The defining apertures were constructed such that the total electron incidence was one hundred and seventy times greater at the cup than at the silicon detector. Thus the cup had a proportionally higher current to measure while the detector was capable of operating in its most efficient range.

The characteristic pulse height spectrum, or count density energy distribution curves, for the detector are shown in Figs. VI and VII, since this spectrum is obtained following amplification of the original signal from the detector, it is characteristic of the amplification technique also. Thus the comparisons made are not universally applicable to the characteristion of this type of detector. The low energy peak of the pulse height spectrum is primarily due to noise, containing a contribution from x-rays, whilst the primary peak is due to electrons. Additional high energy peaks are caused by coincidence counting effects which are usually evident only at very high electron densities.

In order to distinguish the electron counts from the noise, a window is introduced to isolate the primary peak and in order to provide unformity in the standardization, the lower threshold is introduced at the minimum between the first two peaks. Thus although some of the detector's efficiency may be lost, since the rise of the primary peak occurs behind this minima, less indeterminacy is associated with the calibration, since the signal taken from the detector is of electrons only.

The 650 kv Hitachi electron microscope which was utilized for these studies is capable of generating only low beam currents below about 300 kv and at 200 kv, to maintain reasonable electron densities in the image plane, one may not defocus the second condenser lens to any large extent, even at low magnification. The significance of this limitation is that one is unable to satisfactorily defocus out the beam profile across the cup and silicon detector to afford them the same electron incidence, hence the relationship between the cup and detector was not established at this voltage.

The comparisons at 650 kv and 350 kv were more meaningful and the large effects of saturation or coincidence counting in the silicon detector, where the electron incidence is greater than $10^7/cm^2/sec$, were clearly distinguishable. The extent of coincidence counting is however quite predictable (Fig. VIII) and only at incident counts where the random variations ($\sqrt{N}$) approach a significant proportion of the total count (N) at the detector does one observe a marked

uncertainty in the relation. It is noteworthy that the effects of coincidence counting are apparent even at very low counting rates. At 650 kv it is apparent that the detector has, over the lowest range of electron incidence, an efficiency greater than unity. This additional signal from the silicon detector is thought to arise from background X-rays which the faraday cup does not detect.

hus one would expect to be able to calculate the beam current density at the specimen with good accuracy, better than 95%, using either the faraday cup or the lithium drifted silicon detector, if a correction is made for the latter's limited efficiency and the contribution from X-rays is known. The accuracy of the cup itself in detecting electrons is estimated to be better than 99%. The chief error introduced in the calculation of the beam current density at the specimen is due to electrons present in the image plane which are not initiated from the defined area of interest in the specimen. This effect is characteristic of individual microscopes, and must therefore be determined for each specific case.

ACKNOWLEDGEMENTS

The author is grateful for the opportunity to acknowledge the assistance of Mr. W. Toutolmin, who assisted in the design and performed the construction of the Faraday cup, Messers K. Seshan, D. Jurica, J. Wodei and F. Upham for their help and discussion and Mr. W. Chiu for permission to use some of his unpublished results.

The author would also like to express sincere thanks to Dr. G. Thomas and Dr. R. M. Glaeser for their active support and encouragement of this work which he dedicates to his wife Sheila.

This work was done under the auspices of the U. S. Atomic Energy Commission.

REFERENCES

1. H.A. Bethe and W. Heitler, Proc. Roy Soc. London A 146, 83, (1934).
2. H.A. Bethe, Handbook Phys. 24 (1), 273 IV Strosstheorie (1933).
3. F. Bloch, Z. Physik 81, 363, (1933).
4. J.R. Breedlove and G.T. Trammel, Science 190, 1310 (1970).
5. R.E. Burge and E.H. Smith, Proc. Phy. Soc. London 79, 673, (1962).
6. W. Chiu and R.M. Glaeser, to be published.
7. V.E. Cosslett, Proc. 3rd Int. Conf. H.V.E.M. Acad. Press London 147 (1974).
8. R.M. Glaeser, UCRL report No. 2164 (1973).
9. U. Fano, Studies in Penetration of Charged Particles in Matter, Nat. Acad. Sci., 1133 (1964).
10. R.M. Glaeser and L.W. Hobbs, to be published.
11. D.T. Grubb, J. Sci. Inst. 4, 222 (1970).
12. G.L. Jones and V.E. Cosslett, Microscopic Electronique 1, 349 (1970)
13. T.F. Lai, Acta Cryst. (A) 25, S179 (1969).
14. J. Lindhard and Kgl. Scharff, Danske Videnskab, Selskab, Mat-Fys Medd 27 (1953).
15. A.M. Rauth and J.A. Simpson, Radiat Res. 22, 643 (1964).
16. A. Rose, Advan. Electronics, 1, 131 (1948).
17. G. Siegel Z. Natur forsch 27a, 325 (1972).
18. L.I. Schiff, Phys. Rev. 103, 443 (1956).
19. K. Torri and Y. Iitaka, Acta Cryst. (B) 26, 1317 (1970).

Table I.

l-valine	∂E/dx relativistic	∂E/dx non-relativistic	N_{cr}	Average Energy to destroy a molecule	G	$\sigma_d = 1/N_{cr}$	σ_i
650 kv	4.48×10^{6} eV/cm	3.83×10^{6} eV/cm	$6.24\times10^{16}/cm^2$	68.5 eV	1.46	$1.60\times10^{-17}cm^2$	$7.28\times10^{-19}cm^2$
350 kv	5.14×10^{6} eV/cm	4.65×10^{6} eV/cm	$4.99\times10^{16}/cm^2$	75.8 eV	1.59	$2.00\times10^{-17}cm^2$	$8.36\times10^{-19}cm^2$
200 kv	6.37×10^{6} eV/cm	6.00×10^{6} eV/cm	$3.12\times10^{16}/cm^2$	98.02eV	2.05	$3.21\times10^{-17}cm^2$	$1.04\times10^{-18}cm^2$
Adenosine							
650 kv	5.29×10^{6} eV/cm	4.48×10^{6} eV/cm	$3.74\times10^{17}/cm^2$	910 eV	0.11	$2.67\times10^{-18}cm^2$	$9.57\times10^{-19}cm^2$
350 kv	6.04×10^{6} eV/cm	5.44×10^{6} eV/cm	$2.81\times10^{17}/cm^2$	770 eV	0.13	$3.56\times10^{-18}cm^2$	$1.09\times10^{-18}cm^2$
200 kv	7.34×10^{6} eV/cm	6.99×10^{6} eV/cm	$1.75\times10^{17}/cm^2$	590 eV	0.17	$5.71\times10^{-18}cm^2$	$1.32\times10^{-18}cm^2$

where σ_d is the cross section offered by a distinguishable unit of material and σ_i is the cross section offered by one atom.

Plate I. A low resolution electron micrograph of l-valine taken at 650 Kv.

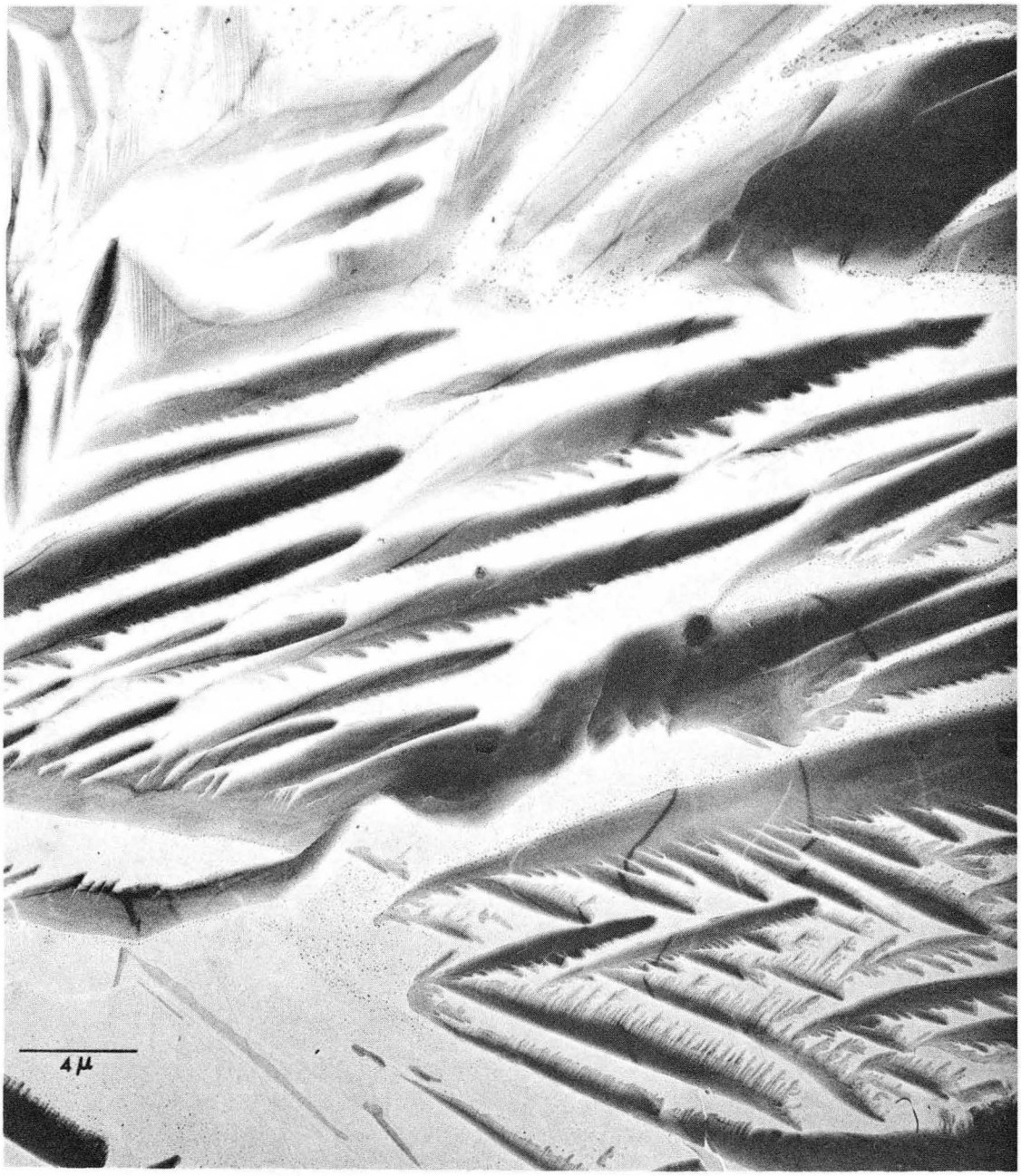

XBB 7311-6800

Plate I.

Plate II. A low resolution electron micrograph of the fibrous structure of adenosine taken at 100 kv.

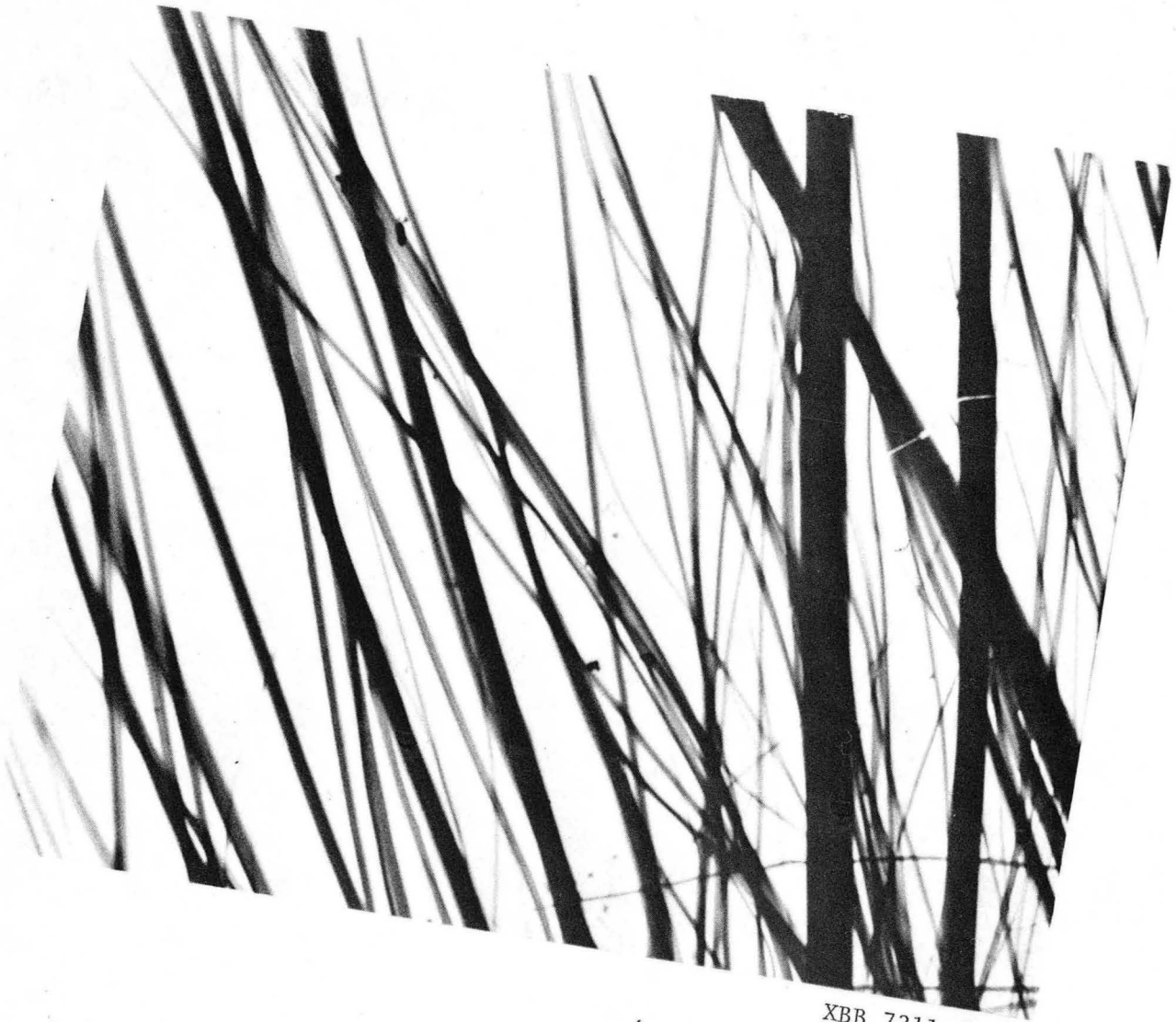

XBB 7311-6798

Plate II.

Plate III. The degradation of a diffraction pattern from l-valine at 650 kv. The recordings were made at approximately equal intervals during the exposure and were not of equivalent optical density.

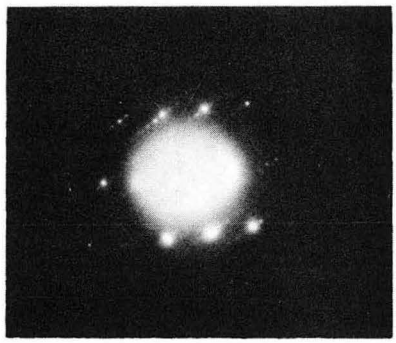

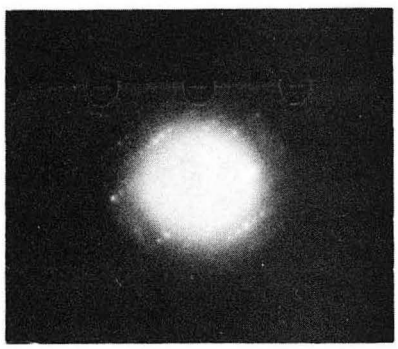

Plate III.

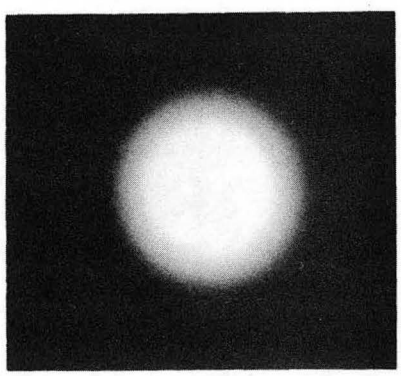

XBB 749--6007

Plate IV. The Faraday cup assembled.

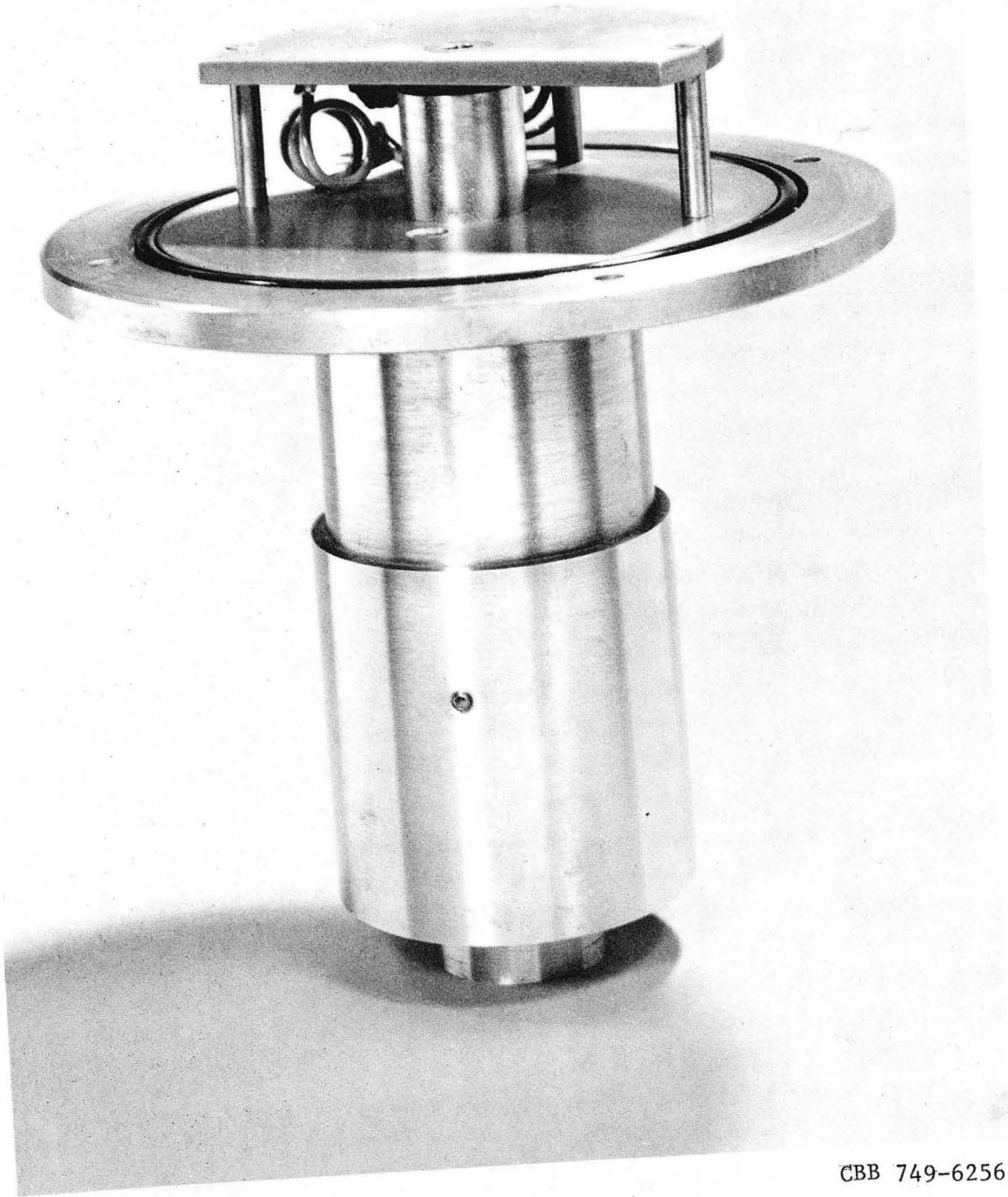

CBB 749-6256

Plate IV.

Plate V. An exploded view of the Faraday cup.

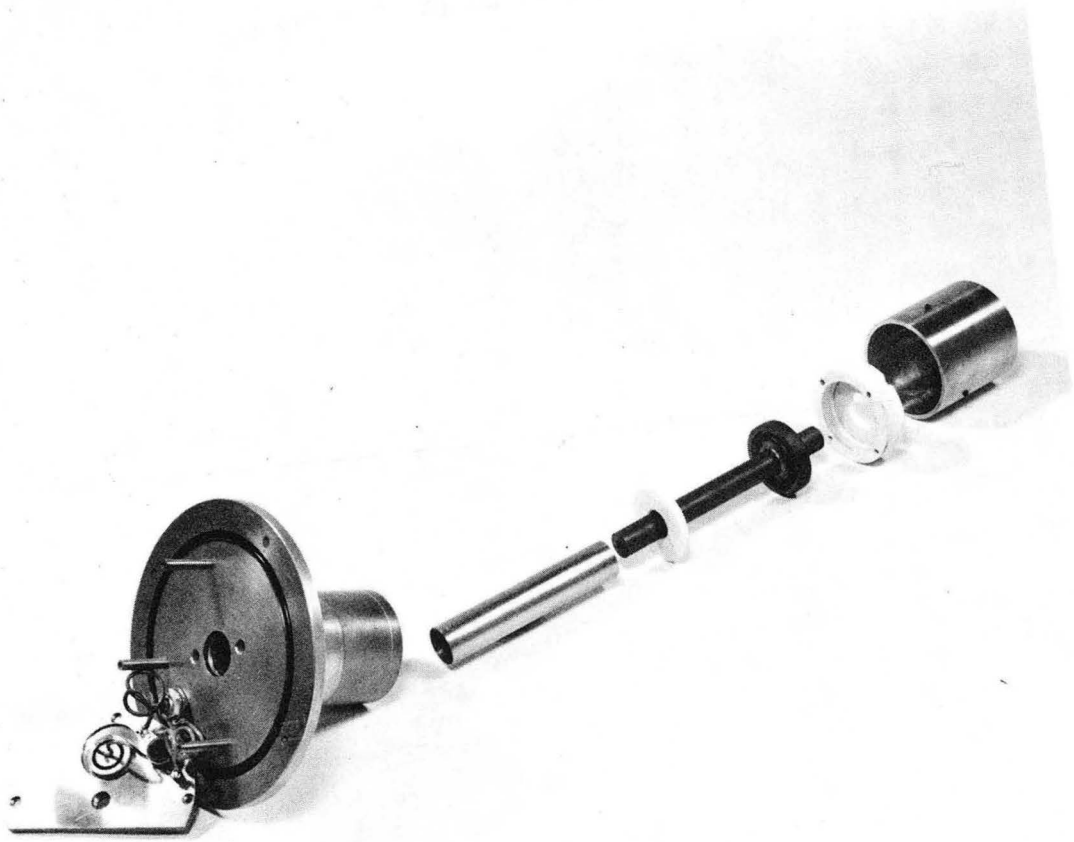

BBC 749-6254

Plate V.

Fig. I. The effects of additional electron incidence upon the variation of the accuracy of the beam current density measurement with magnification in the 650 Kv Hitachi microscope. The broadening of the curves represents the uncertainty in the measurements.

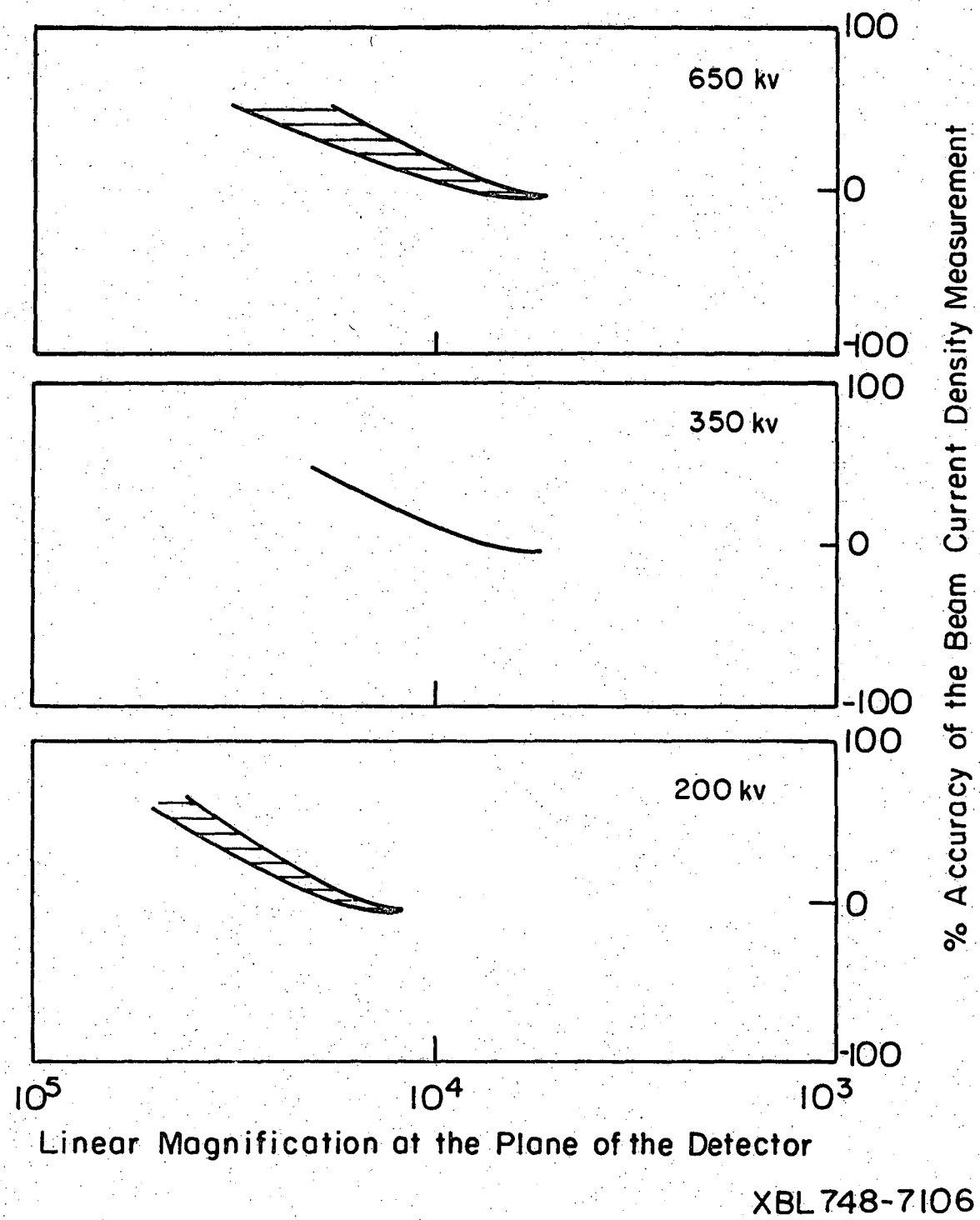
650 kv
350 kv
200 kv
100
0
-100
% Accuracy of the Beam Current Density Measurement
10^5
10^4
10^3
Linear Magnification at the Plane of the Detector
XBL 748-7106

Fig. I.

Fig. II. The variation of specimen lifetime with dose rate in adenosine and l-valine at 200 Kv.

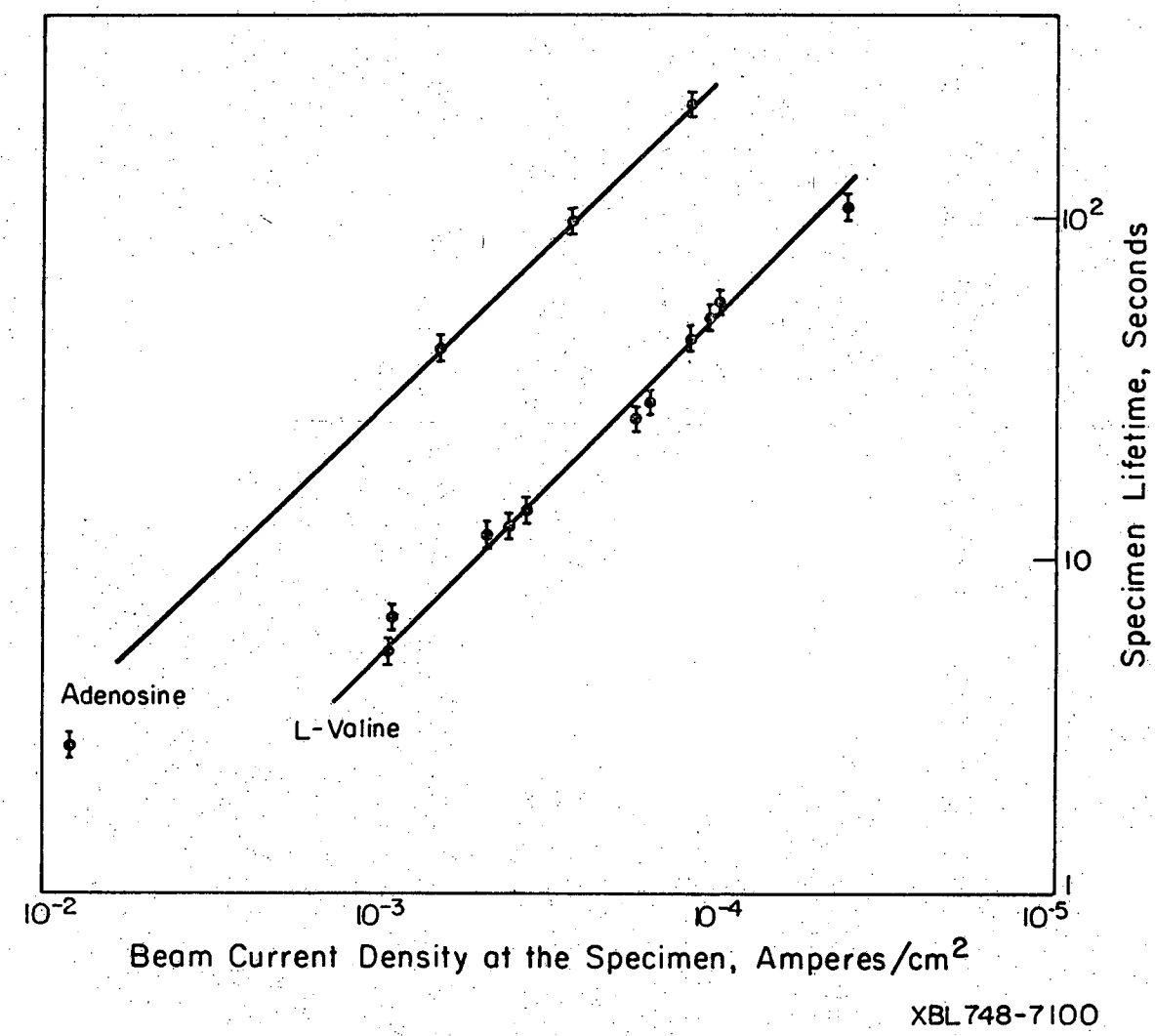
Adenosine
L-Valine
10^{2}
10
1
10^{-2}
10^{-3}
10^{-4}
10^{-5}
Specimen Lifetime, Seconds
Beam Current Density at the Specimen, Amperes/cm^2
XBL748-7100

Fig. II.

Fig. III. The variation of specimen lifetime with dose rate in adenosine and l-valine at 350 Kv.

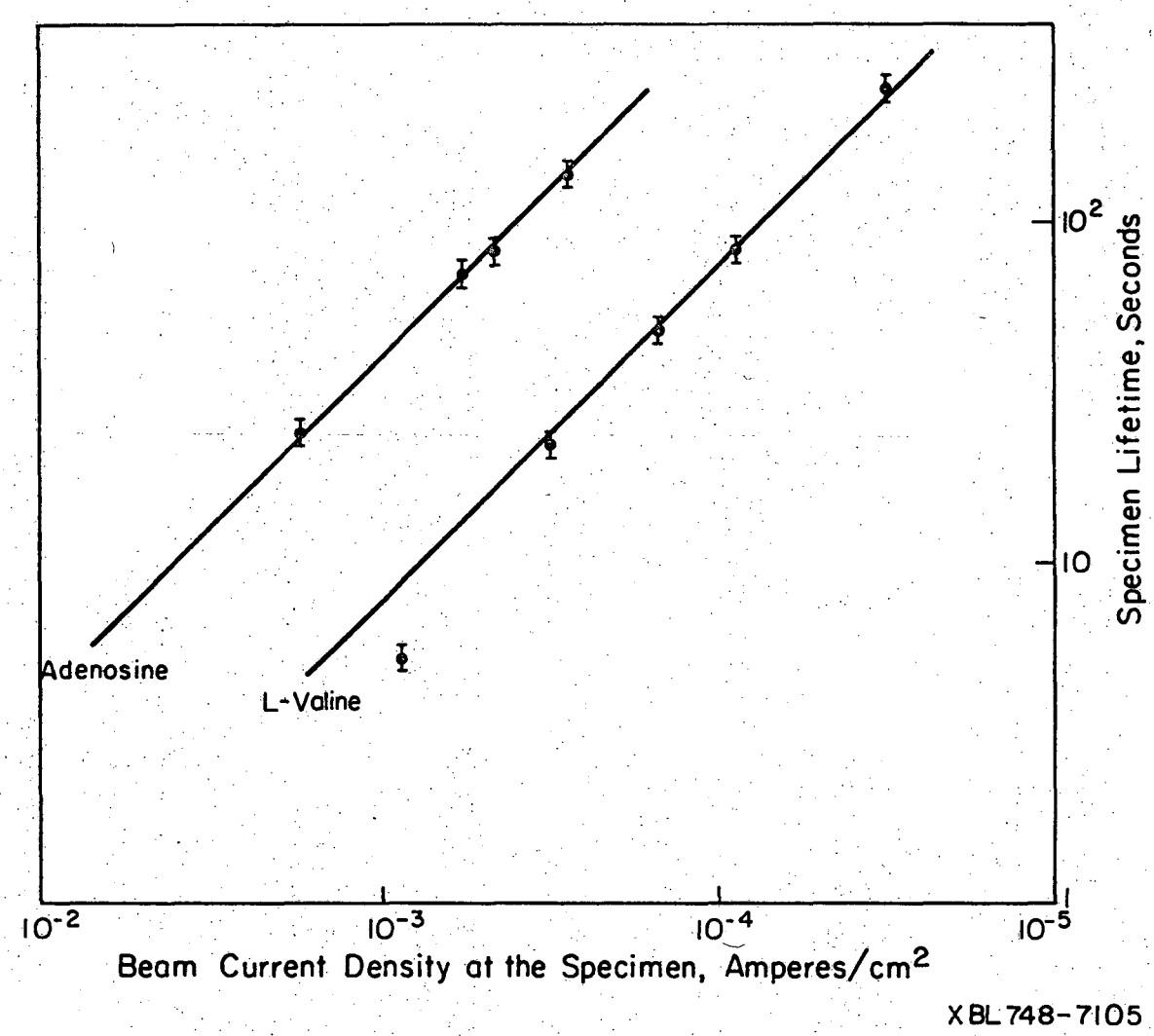
Adenosine
L-Valine
10^2
10
Specimen Lifetime, Seconds
10^{-2}
10^{-3}
10^{-4}
10^{-5}
Beam Current Density at the Specimen, Amperes/cm^2
XBL748-7105

Fig. III.

Fig. IV. The variation of specimen lifetime with dose rate in adenosine and l-valine at 650 Kv.

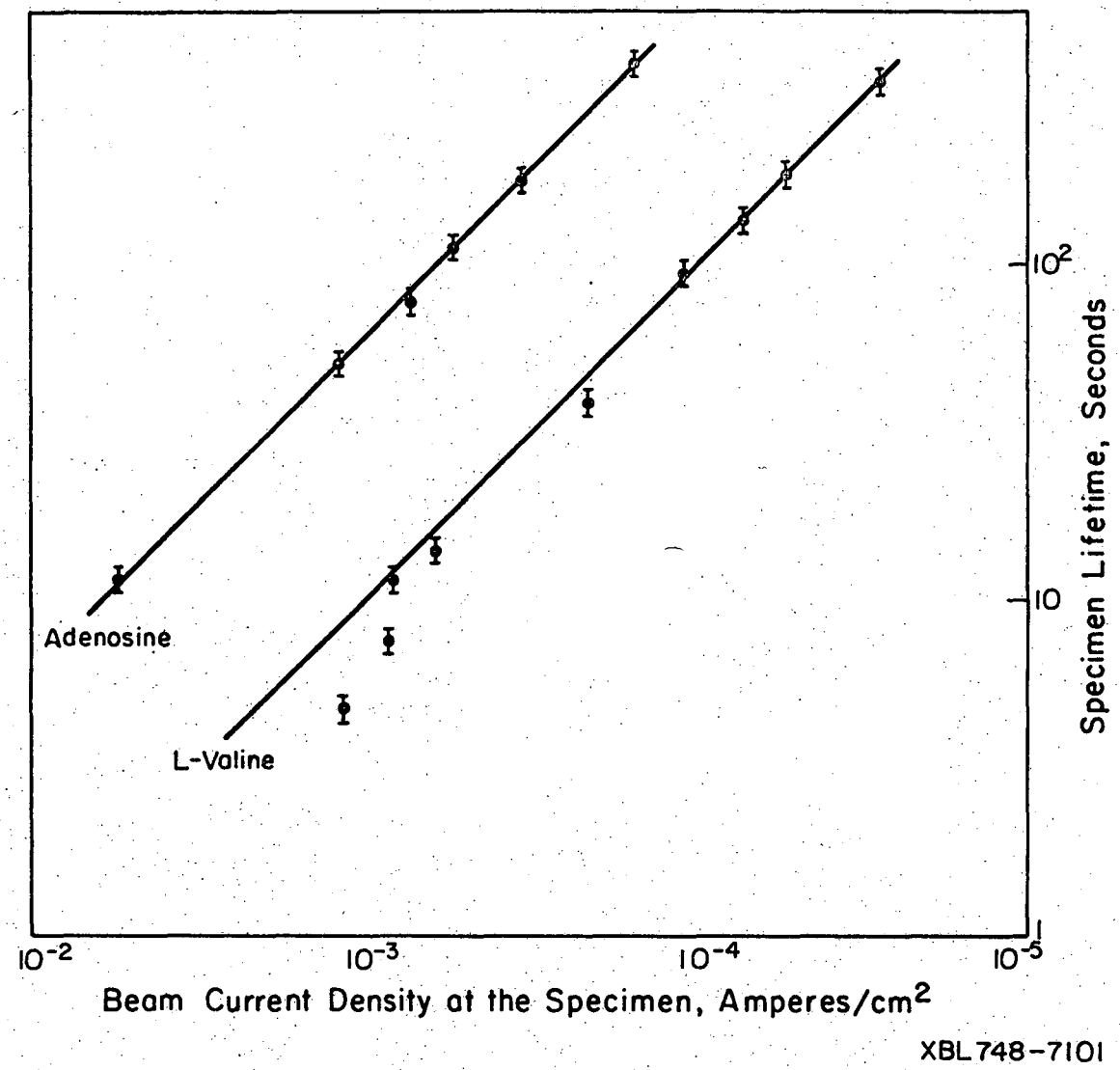
Adenosine
L-Valine
10^{2}
10
1
Specimen Lifetime, Seconds
10^{-2}
10^{-3}
10^{-4}
10^{-5}
Beam Current Density at the Specimen, Amperes/cm^2
XBL748-7101

Fig. IV.

Fig. V. The variation of critical exposure of adenosine and l-valine with the velocity of the irradiating electrons. The broken line indicates the behavior consistent with stopping power theory and a single hit target model.

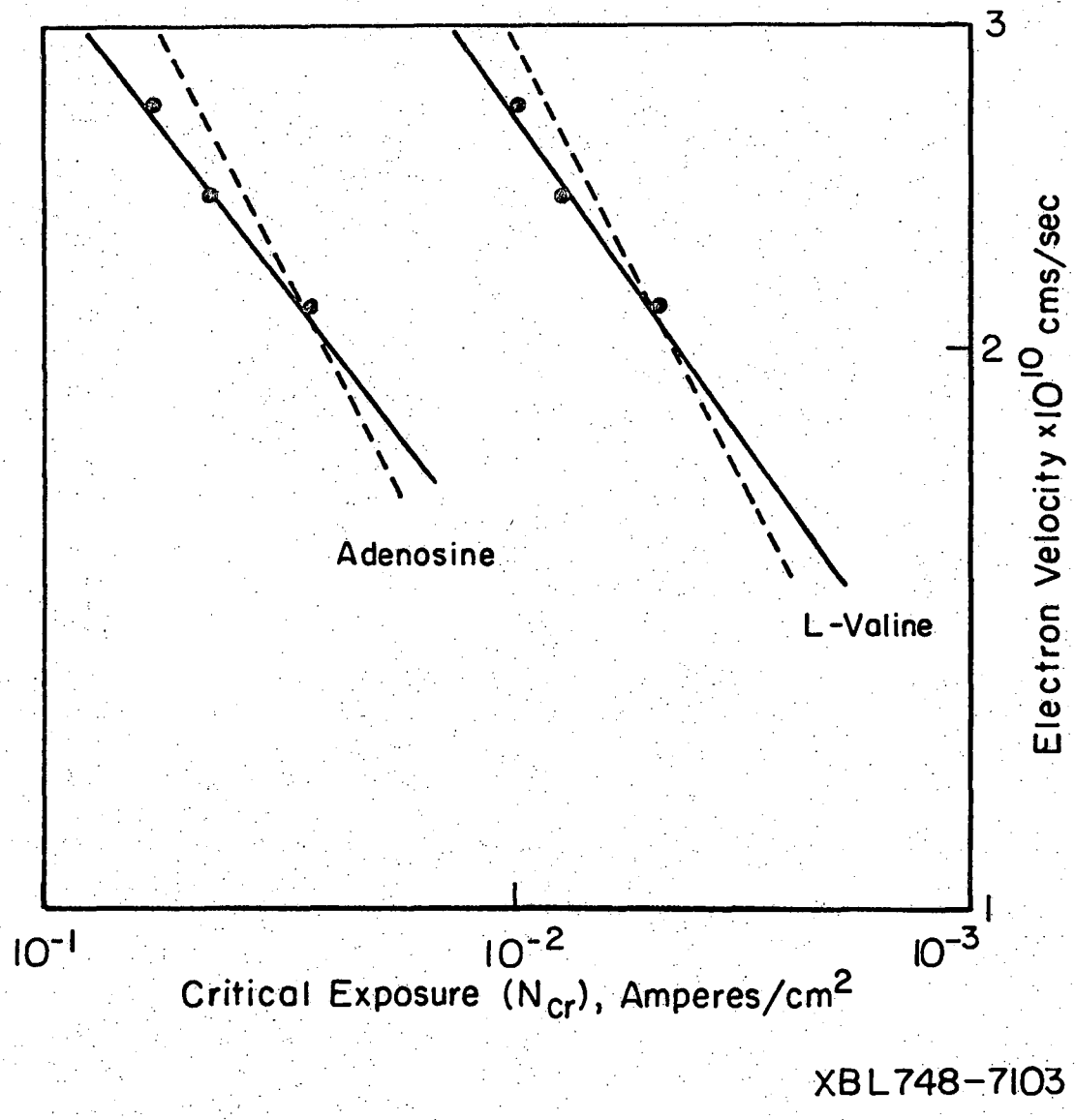
3
2
1
Electron Velocity x10^10 cms/sec
Adenosine
L-Valine
10^-1
10^-2
10^-3
Critical Exposure (N_cr), Amperes/cm^2
XBL748-7103

Fig. V.

Fig. VI. The pulse height spectrum or energy distribution of signal from the lithium drifted silicon detector at 350 kv. The measurements were made by scanning the total energy range of the analyser window at 0.02 volt intervals.

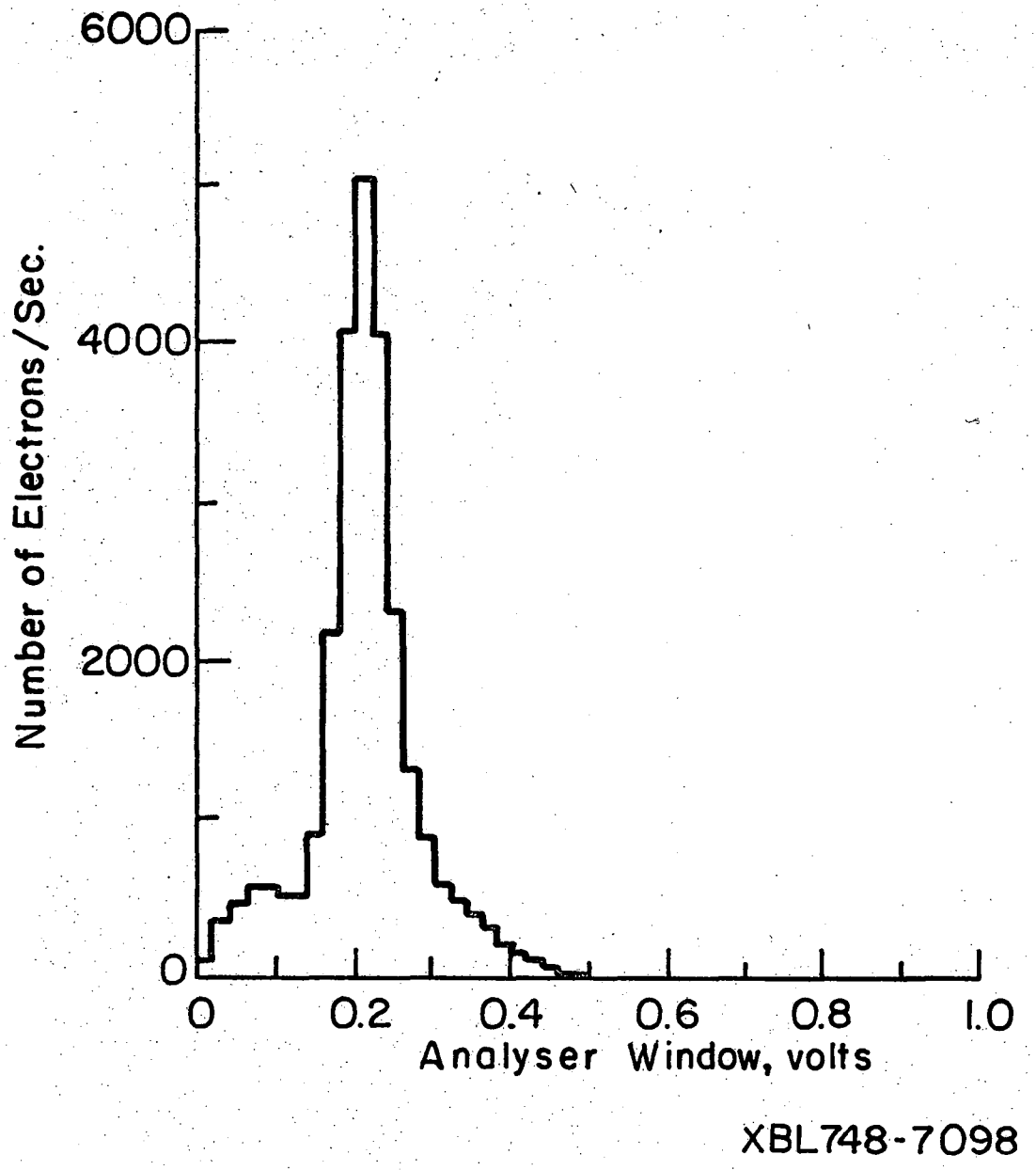
6000
4000
2000
0
Number of Electrons/Sec.
0
0.2
0.4
0.6
0.8
1.0
Analyser Window, volts
XBL748-7098

Fig. VI.

Fig. VII. The pulse height spectrum or energy distribution of signal from the lithium drifted silicon detector at 650 kv. The measurements were made by scanning the total energy range of the analyser window at 0.02 volt intervals.

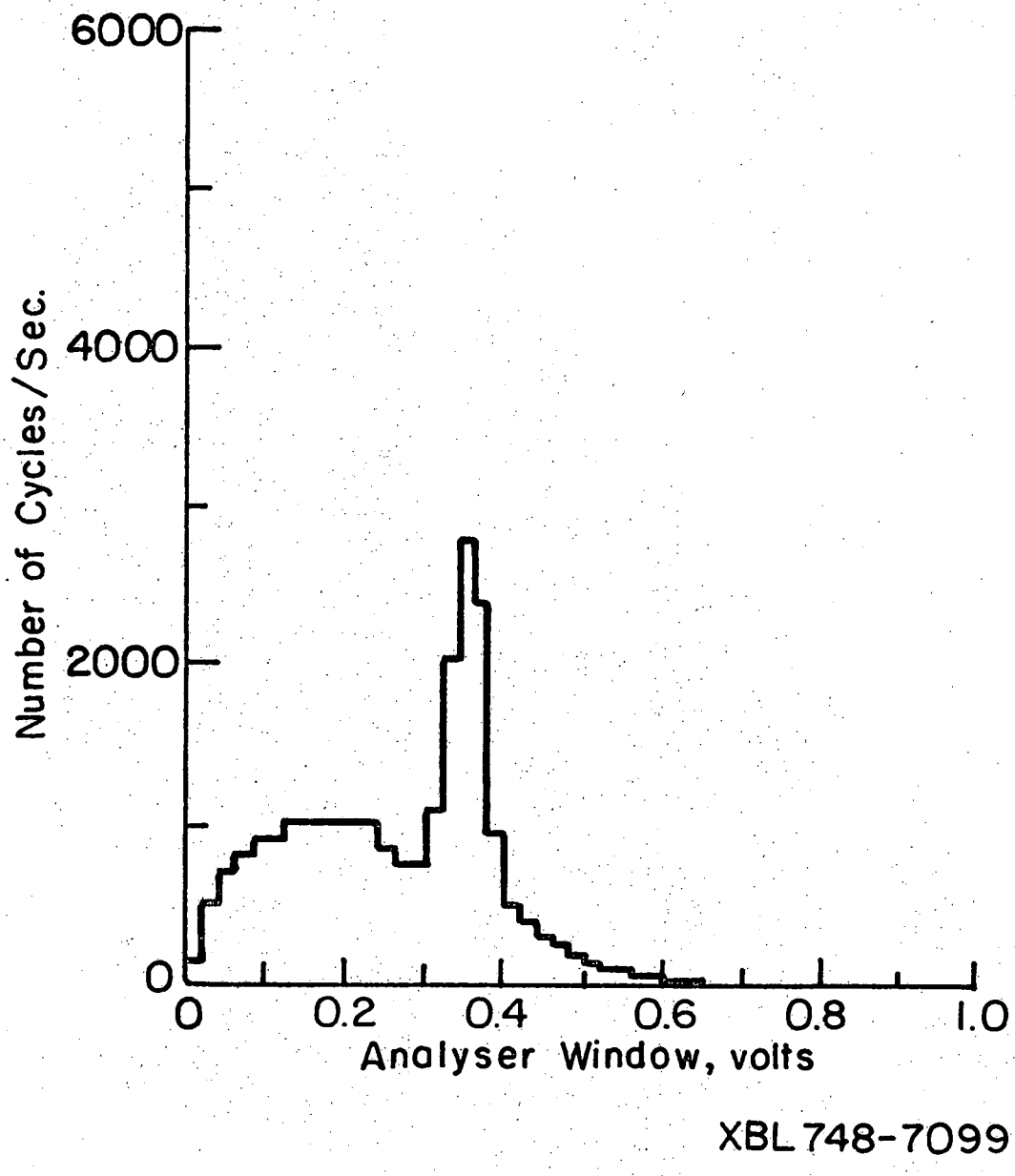
6000
4000
2000
0
Number of Cycles/Sec.
0
0.2
0.4
0.6
0.8
1.0
Analyser Window, volts
XBL 748-7099

Fig. VII.

Fig. VIII. The relation between the efficiency of the lithium drifted silicon detector and the electron incidence measured by it. The conversion from electron density at the detector to the detectors actual count rate is for the defining aperture used (0.0368 cms diameter).

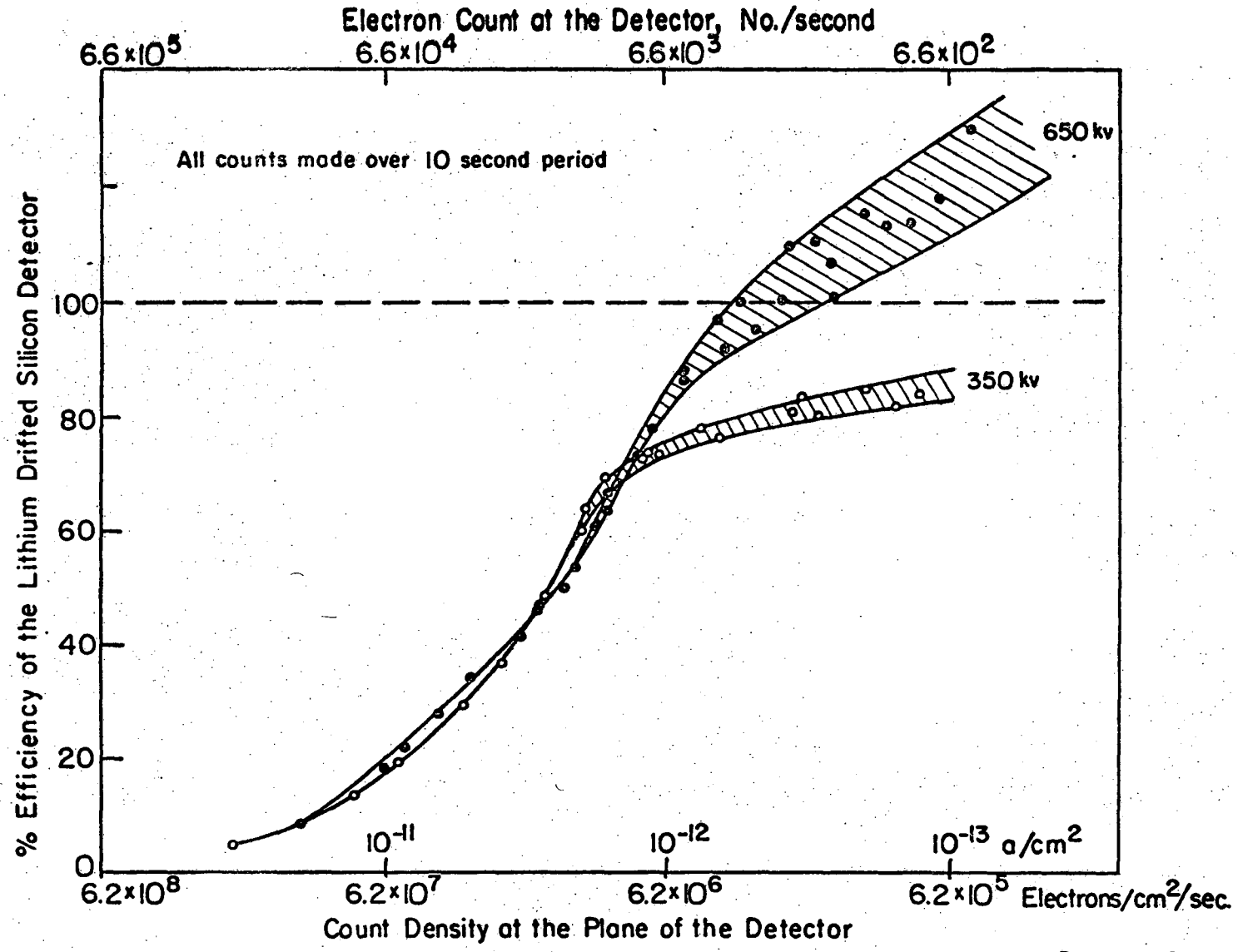
Electron Count at the Detector, No./second
6.6x10^5
6.6x10^4
6.6x10^3
6.6x10^2
All counts made over 10 second period
650 kv
350 kv
% Efficiency of the Lithium Drifted Silicon Detector
100
80
60
40
20
0
10^-11
10^-12
10^-13 a/cm^2
6.2x10^8
6.2x10^7
6.2x10^6
6.2x10^5 Electrons/cm^2/sec.
Count Density at the Plane of the Detector
XBL748-7104

Fig. VIII.

TECHNICAL INFORMATION DIVISION
LAWRENCE BERKELEY LABORATORY
UNIVERSITY OF CALIFORNIA
BERKELEY, CALIFORNIA 94720